npj | precision oncology

Article

Published in partnership with The Hormel Institute, University of Minnesota

https://doi.org/10.1038/s41698-024-00729-0

Genomic and transcriptomic analyses identify distinctive features of triple-negative inflammatory breast cancer

Xiaoping Wang[1,2,3,8] ✉, Li Zhao[4,8], Xingzhi Song[4], Xiaogang Wu[4], Savitri Krishnamurthy[1,5], Takashi Semba[1,2], Shan Shao[1,2], Mark Knafl[4], Larry W. Coffer II[1,2], Angela Alexander[1,2], Anita Vines[1,2], Swetha Bopparaju[1,2], Wendy A. Woodward[1,6], Randy Chu[4], Jianhua Zhang[4], Clinton Yam[2], Lenora W. M. Loo[3], Azadeh Nasrazadani[1,2], Le-Petross Huong[1,7], Scott E. Woodman[4], Andrew Futreal[4], Rare Tumor Initiative Team*, Debu Tripathy[2] & Naoto T. Ueno[1,2,3] ✉

Triple-negative inflammatory breast cancer (TN-IBC) is the most aggressive type of breast cancer, yet its defining genomic, molecular, and immunological features remain largely unknown. In this study, we performed the largest and most comprehensive genomic and transcriptomic analyses of prospectively collected TN-IBC patient samples from a phase II clinical trial (*ClinicalTrials.gov, NCT02876107, registered on August 22, 2016*) and compared them to similarly analyzed stage III TN-non-IBC patient samples (*ClinicalTrials.gov, NCT02276443, registered on October 21, 2014*). We found that TN-IBC tumors have distinctive genomic, molecular, and immunological characteristics, including a lower tumor mutation load than TN-non-IBC, and an association of immunosuppressive tumor-infiltrating immune components with an unfavorable response to neoadjuvant chemotherapy. To our knowledge, this is the only study in which TN-IBC and TN-non-IBC samples were collected prospectively. Our analysis improves the understanding of the molecular landscape of the most aggressive subtype of breast cancer. Further studies are needed to discover novel prognostic biomarkers and druggable targets for TN-IBC.

Inflammatory breast cancer (IBC) is the most lethal and aggressive form of breast cancer[1], with over 40% of patients presenting with stage IV disease at diagnosis. IBC accounts for 2–4% of breast cancer cases but causes 8% to 10% of breast cancer deaths. The diagnosis of IBC is based on clinical characteristics, including erythema, edema, and/or "orange peel" appearance of the breast with rapid onset of symptoms. Although trimodality therapy consisting of chemotherapy, surgery, and radiation therapy has significantly improved patient survival, the 5-year survival rate for IBC patients is an abysmal 40% (compared to 90% for non-IBC patients)[2–4]. Like non-IBC, IBC is composed of different subtypes based on the expression status of estrogen receptor (ER), progesterone receptor (PR), and HER2. The triple-negative subtype of IBC (TN-IBC) lacks expression of ER, PR, and HER2, representing about 20% to 40% of IBC cases. It is associated with worse overall survival (OS) and disease-free survival than IBC that is positive for ER, PR, and/or HER2[5].

An immune checkpoint inhibitor, the anti-PD-1 antibody pembrolizumab, plus neoadjuvant chemotherapy (NAC) has become a frontline treatment for patients with early-stage triple-negative breast cancer (TNBC), including TN-IBC[6]. However, TN-IBC patients often have a suboptimal response to this regimen likely due in part to the immunosuppressive tumor microenvironment (TME). There is a critical need to develop novel therapeutic

[1]Morgan Welch Inflammatory Breast Cancer Research Program and Clinic, The University of Texas MD Anderson Cancer Center, Houston, TX, USA. [2]Department of Breast Medical Oncology, The University of Texas MD Anderson Cancer Center, Houston, TX, USA. [3]University of Hawai'i Cancer Center, Honolulu, HI, USA. [4]Department of Genomic Medicine, The University of Texas MD Anderson Cancer Center, Houston, TX, USA. [5]Department of Pathology, The University of Texas MD Anderson Cancer Center, Houston, TX, USA. [6]Department of Breast Radiation Oncology, The University of Texas MD Anderson Cancer Center, Houston, TX, USA. [7]Department of Breast Imaging, The University of Texas MD Anderson Cancer Center, Houston, TX, USA. [8]These authors contributed equally: Xiaoping Wang, Li Zhao. *A list of authors and their affiliations appears at the end of the paper. ✉e-mail: xiaopingwang@cc.hawaii.edu; nueno@cc.hawaii.edu

approaches by identifying targetable molecules in both tumor cells and TME components for patients with TN-IBC.

Over the past 2 decades, there have been extensive efforts to identify the genomic and molecular signatures of IBC. Genomic profiling of IBC, including targeted next-generation sequencing, whole-exome sequencing (WES)[7], and whole-genome sequencing[8], has identified several genomic alterations, including alterations in *TP53*[9–14], *PIK3CA*[7,12–15], *ERBB2/HER2*[11,13–15], *MYC*[14,15], *BRCA2*[12,14,15], *NOTCH1*[15], *NOTCH2*[12], and *NOTCH4*[12]. Some molecular changes in IBC patient samples are associated with the aggressiveness of IBC, including overexpression of NF-κB target genes[16–18], activation of the JAK/STAT pathway[19], attenuation of TGF-β signaling[20], and up-regulation of transcription factors (*JUN, EGR1, JUNB*, etc.)[21], growth factors (*VEGF, IL6, EREG, CCL3, CCL5*, etc.)[21], and growth factor receptors (*TBXA2R, TNFRSF10A/TRAILR1*, and *ROBO2*)[21]. In addition, a 109-gene expression signature and a 79-gene signature were reported to distinguish IBC from non-IBC samples[9,20]. Yet despite these extensive efforts, very few genes were identified and validated across studies, and we are aware of no published genomic and molecular profiling studies focused on TN-IBC samples.

In addition to genomic and molecular signatures, TME components may distinguish IBC from non-IBC. Specifically, T cells, tumor-associated macrophages, fibroblasts, mast cells, and mesenchymal stem cells have emerged as critical drivers of the IBC clinical phenotype and aggressiveness[22–24]. We also demonstrated that tumor-infiltrating lymphocytes (TILs) are increased in tumors of patients with pathologic complete responses (pCR) to NAC[25]. These findings suggest that tumor immune signatures may distinguish IBC from non-IBC cases. However, such information is not available yet for patients with TN-IBC.

To identify distinctive genomic and molecular features of TN-IBC, we performed comprehensive genomic and transcriptomic analyzes of TN-IBC patient samples collected from a phase II clinical trial (NCT02876107) in which patients were treated with NAC alone or the anti-EGFR antibody panitumumab (PmAb) combined with NAC (PmAb/NAC). Specifically, we (i) examined germline and somatic alterations, gene expression profiles, and tumor-infiltrating immune cells in the TN-IBC samples, (ii) identified distinctive features of TN-IBC by comparing TN-IBC patient samples with similarly analyzed stage III TN-non-IBC patient samples, and (iii) explored the genomic, molecular, and immune features that may be associated with response of TN-IBC to NAC and PmAb/NAC.

Methods

Study design and patients

The design of the study (ClinicalTrials.gov Identifier: NCT02876107, registered on August 22, 2016) is shown in Supplementary Fig. 1. This is a randomized phase II trial to determine the pCR rate in patients with primary TN-IBC treated with PmAb, carboplatin, and paclitaxel followed by standard-of-care doxorubicin and cyclophosphamide (AC), termed PmAb/NAC, or carboplatin and paclitaxel followed by AC, termed NAC, as neoadjuvant therapy. The study was approved by the Institutional Review Board (IRB) of The University of Texas MD Anderson Cancer Center (IRB reference number: PA12-0305), in accordance with the ethical standards of the 1964 Declaration of Helsinki and its subsequent amendments. Written informed consent, including consent for data publication, was obtained from all participants prior to their inclusion in the study. Seventy-two patients with primary TN-IBC were planned to be recruited and randomized into the PmAb/NAC and NAC arms. As of this writing, 42 patients with primary TN-IBC have enrolled in the study. Written informed consent was obtained from all patients.

IBC specialists reviewed all cases in a prospective manner. Patient inclusion criteria include: (1) Patients must have histological confirmation of breast carcinoma. (2) Patients must have IBC confirmed according to international consensus criteria including (i) Onset: Rapid onset of breast erythema, edema, and/or peau d'orange, and/or warm breast, with or without an underlying breast mass (ii) Duration: History of such findings no more than 6 months (iii) Extent: Erythema occupying at least 1/3 of whole breast (iv) Pathology: Pathologic confirmation of invasive carcinoma. (3) Patients must have an Eastern Cooperative Oncology Group (ECOG) performance status of 0–1. (4) Patients must have negative HER2 expression on immunohistochemistry (IHC) or fluorescence in situ hybridization (FISH) analysis; ER and PR expression should be less than 10%.

In the PmAb/NAC arm, patients received an initial dose of PmAb, followed by weekly PmAb and paclitaxel and triweekly carboplatin for 4 cycles. Tissue biopsy was performed before and after the initial dose of PmAb. In the NAC arm, patients received the same chemotherapy without PmAb. Tissue biopsy was performed only at baseline. Each cycle was defined as 21 days. Standard-of-care chemotherapy (doxorubicin and cyclophosphamide) was administered after completion of PmAb/NAC or NAC. The doxorubicin and cyclophosphamide regimen consisted of 4 cycles repeated at 2- to 3-week intervals at the physician's discretion, assuming bone marrow recovery. Dose modification of doxorubicin and cyclophosphamide was based on standard practice guidelines.

Modified radical mastectomy was performed after systemic therapy, and board-certified breast pathologists determined the residual cancer burden. pCR was defined as no invasive carcinoma in the breast, skin, and axillary lymph nodes and no tumor emboli within the surgical pathology specimen[26].

From August 2016 through July 2022, 42 patients with primary TN-IBC were enrolled and randomized 1:1 into the PmAb/NAC or NAC arm. Baseline tumor samples of 19 patients, 8 in the PmAb/NAC arm and 11 in the NAC arm, were collected for molecular profiling.

Whole-exome sequencing

Genomic DNA from 19 tumor tissues and matched blood samples was extracted with the Biospecimen Extraction Resource of MD Anderson Cancer Center. Genomic DNA from matched blood samples were used as germline controls. 500 ng of DNA per sample was proceeded to library preparation using Roche KAPA library prep kit (KAPA) following manufacturer's "with beads" protocol (KAPA Biosystems, Wilmington, MA). Exome capture was performed using whole exome biotin labeled probes from Agilent SureSelect Human All Exon V4 by following manufacture's protocol. WES was performed on the Illumina HiSeq 2500 sequencing platform. Pair-end sequencing reads in FASTQ format were generated from BCL raw data using Illumina CASAVA 1.8.2. The reads were aligned to the hg19 human reference genome using BWA 0.7.3[27]. The duplicate reads were removed using Picard 2.1.1 (unpublished, http://broadinstitute.github.io/picard/), and local realignments were performed using the GATK 4.0.1[28]. The BAM files were then used for downstream analysis.

Variant calling and CNV identification

Platypus[29] was used to call germline variants on breast cancer susceptibility genes and TGF-β genes. MuTect[30] was used to identify somatic point variants, and Pindel[31] was used to identify somatic insertions and deletions. A series of post-calling filters was applied for somatic mutations, including (a) total read count in tumor sample ≥20, (b) total read count in germline sample ≥10, (c) variant allele frequency ≥0.02 in tumor sample and ≤0.02 in matched normal sample, and (d) population frequency of <1% in the databases of dbSNP129[32], 1000 Genomes Project[26], Exome Aggregation Consortium[33], and ESP6500[34], used to filter out common variants. To understand the potential functional consequences of detected variants, we annotated them using Annovar[35] and dbNSFP[36] and compared them with the dbSNP[37], ClinVar[38], COSMIC[39], and TCGA databases.

Copy number variations (CNVs) were identified using an in-house algorithm, ExomeCN. The copy number $\log_2$ tumor versus matched normal ratios were calculated across the entire capture regions and then subjected to segmentation using CBS[40]. A cutoff of $\log_2$ ratio ≤−0.4 was applied to identify copy losses, and $\log_2$ ratio ≥0.4 was applied to identify copy gains.

RNA sequencing

Total RNA from tumor tissues from the 19 patients was extracted and prepared using Agilent SureSelect probes following the manufacturer's

protocol. RNA sequencing was conducted on the Illumina NovaSeq 6000 platform. Raw sequencing data were converted to FASTQ files and aligned to the reference genome (hg19) using the Spliced Transcripts Alignment to a Reference algorithm field[41]. HTSeq-count was then utilized to generate the raw read counts for each gene[42]. DESeq2 1.38.3 was used for data processing, normalization, and differential expression analysis following standard procedures[43]. The differentially expressed genes were selected by the $\log_2$(fold change) (Log2FC) criteria ≤−1 or ≥1, and the cutoff of adjusted *p*-value (adj-*p*) was 0.05. Gene Set Variation Analysis (GSEA 1.46.0)[33,44] was used to estimate the variation of gene set enrichment across TN-IBC samples, and the normalized enrichment score (NES) was used to quantify the enrichment. The Molecular Signatures Database hallmark gene set collection[34,45] was used in pathway analysis. CIBERSORT[46] was used to perform deconvolution analysis to estimate the composition of tumor infiltrating immune cells.

Comparison between pCR and non-pCR groups

Patients were classified into 2 groups according to their pathologic response: pCR and non-pCR. The pCR and non-pCR groups were compared in the NAC and PmAb/NAC arms separately. To enrich sample size, we also compared patients who achieved a pCR from the NAC arm only with patients who did not achieve a pCR from both arms. Patients who achieved a pCR from the PmAb/NAC arm were excluded to eliminate the potential effect of PmAb on patient response.

TN-non-IBC cohort

A pretreatment TN-non-IBC cohort was selected from the ARTEMIS clinical trial (ClinicalTrials.gov Identifier: NCT02276443, registered on October 21, 2014), an ongoing clinical trial evaluating targeted NAC in chemotherapy-insensitive TNBC. The ARTEMIS study protocol was reviewed by The University of Texas MD Anderson Cancer Center IRB and all patients provided informed consent. All study procedures performed were in accordance with ethical standards of the IRB and with the 1964 Helsinki declaration and its later amendments or comparable ethical standards. In brief, treatment-naïve patients with operable TNBC planned for NAC with an anthracycline/taxane-based regimen were enrolled. All patients underwent a pretreatment biopsy of the breast tumor. The results of the molecular characterization from the pretreatment biopsy were used in combination with response assessment after 4 cycles of doxorubicin and cyclophosphamide to identify chemotherapy-insensitive disease. Patients with chemotherapy-sensitive disease were recommended to continue doxorubicin and cyclophosphamide for the second phase of treatment. Patients with chemotherapy-insensitive disease were offered therapy on clinical trials using targeted therapy based on specific molecular characteristics in combination with chemotherapy. Upon completion of the second phase of treatment, patients underwent surgical resection, and residual cancer burden was determined.

For comparison with the TN-IBC cohort, we selected patients with TN-non-IBC from the ARTEMIS trial according to the following criteria: (i) Only patients with TN-non-IBC were included. (ii) As TN-IBC is very aggressive, at the time of diagnosis, TN-IBC is either stage III or stage IV. Therefore, to make a fair comparison with TN-non-IBC, only patients with stage III or IV TN-non-BC were included. Stage IV refers to those spread beyond the breast and nearby lymph nodes to other distant organs. (iii) Patients who received targeted therapy in the second phase of treatment and achieved a pCR were excluded. (iv) To minimize the sequencing batch effect, only patients who had sequencing using the same protocol and same platform as the TN-IBC cohort were included. With these criteria, from among the patients with TN-non-IBC in ARTEMIS, we selected 60 patients with WES data and 19 patients with RNA-seq data for comparison with the TN-IBC cohort.

Statistical analysis

To evaluate statistical significance, a Student *t*-test was used if the data fit the normal distribution. Otherwise, the Wilcoxon rank-sum test was used to test the differences between groups. The Benjamini–Hochberg method was used to control the false discovery rate. In transcriptomic analysis, the differential expression was evaluated using a negative binomial generalized linear model described in DESeq2[43], and logarithmic fold change and adjusted *p*-values (adj-*p*) were used for differentially expressed gene assessment.

Table 1 | Baseline characteristics of 19 patients with TN-IBC

Characteristic	Value
Age, mean (SD) range, y	52.7 (13.0) 31–72
BMI, mean (SD) range, kg/m^2	33.9 (10.1) 20.4–59.6
TILs, mean (SD) range, %	35.7 (30.2) 1–80
Menopausal status, *n* (%)	
Premenopausal	8 (42)
Postmenopausal	11 (58)
Race, *n* (%)	
American Indian or Alaska Native	1 (5)
Asian	2 (11)
Black or African American	3 (16)
White or Caucasian	13 (68)
Ethnicity, *n* (%)	
Hispanic or Latino	2 (11)
Not Hispanic or Latino	17 (90)
Clinical stage	
IIIB	8 (42)
IIIC	9 (47)
IV	2 (11)
N category at diagnosis	
N0	1 (5)
N1	6 (32)
N2a	2 (11)
N3a	4 (21)
N3b	2 (11)
N3c	4 (21)

BMI body mass index, *SD* standard deviation, *TIL*s tumor-infiltrating lymphocytes.

Results

Characteristics of the patients with TN-IBC

The baseline clinical characteristics of the 19 patients with TN-IBC included in this analysis are shown in Table 1. The mean age was 52.7 years (range, 31–72). Eight patients (42%) were premenopausal, and 11 (58%) had reached menopause. The mean body mass index (BMI) at the time of diagnosis was 33.9 kg/m^2 (range, 20.4–59.6). The self-reported race was White or Caucasian for 13 patients, Black or African American for 3, Asian for 2, and American Indian or Alaska Native for 1. Eight patients (42%) had stage IIIB disease, 9 (47%) had stage IIIC disease, and 2 (11%) had stage IV metastatic disease. The mean TIL percentage was 35.7% (range, 1–80%). We also compared the clinical characteristics of 19 TN-IBC patients with 60 TN-non-IBC patients (Supplementary Table 1). We observed higher BMI in TN-IBC compared to TN-non-IBC (mean: 33.9 kg/m^2 vs 28.9 kg/m^2, $p = 0.05$).

Germline and somatic mutations in TN-IBC

We first isolated germline DNA from TN-IBC peripheral blood samples and sequenced the DNA to assess the germline variants. The mean coverage for germline WES data was 155×. We identified a mean of 90 nonsynonymous germline variants per patient, including 63 missense variants, 20 truncating variants, and 7 inframe indels. Next, we analyzed oncogenic pathways

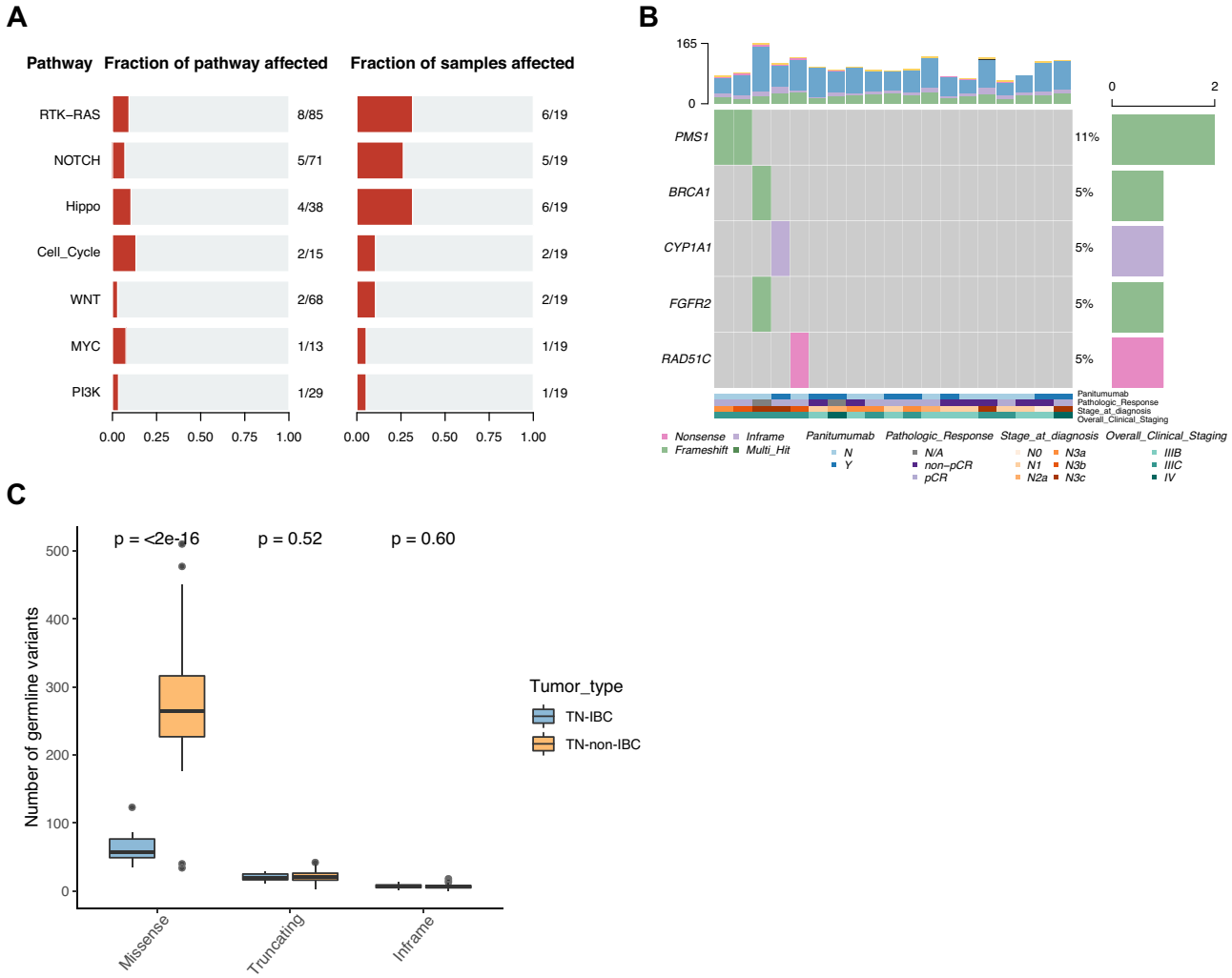

Fig. 1 | Germline mutations identified in TN-IBC and comparison with TN-non-IBC. A Altered oncogenic pathways affected by germline mutations in TN-IBC. **B** Germline mutations of breast cancer susceptibility genes in TN-IBC. Top: bar graph defining the total number of different types of germline mutations in each patient; bottom: annotation for PmAb treatment, pathologic response, stage at diagnosis, and overall clinical stage. **C** Number of germline variants, including missense, truncating, and inframe, in TN-IBC and TN-non-IBC samples. In this boxplot, the center line represents the median of the data. The edges of the box correspond to the 75th percentile and the 25th percentile respectively, showing the interquartile range (IQR). The whiskers extend to the largest and smallest values within 1.5 times the IQR from the 25th and 75th percentiles. Outliers, defined as data points beyond the whiskers, are plotted individually as dots.

affected by these germline variants and found that the RTK-RAS pathway (6 patients, 32%), Hippo pathway (6, 32%), and NOTCH pathway (5, 26%) were the most frequently altered pathways (Fig. 1A). We further found that 5 of 19 patients (26%) had putative deleterious mutations in 40 breast cancer susceptibility genes, including *PMS*1 (2 patients, 11%), *BRCA1* (1, 5%), *CYP1A1* (1, 5%), *FGFR2* (1, 5%) and *RAD51C* (1, 5%) (Fig. 1B).

Next, we analyzed the somatic mutations in these TN-IBC tumor samples by comparing the tumor samples to the matched blood samples. We identified a mean of 96 nonsynonymous somatic mutations and 37 CNVs per sample. We plotted the somatic alteration landscape based on a known list of breast cancer driver genes and cancer hallmark genes (https://cancer.sanger.ac.uk/census). As shown in Fig. 2A, 34 breast-cancer-associated genes were altered in 17 of 19 TN-IBC patients. Most alterations in these 34 genes were deletion mutations (present in 15 patients, 79%) and the most frequently altered genes were *TP53* (8 patients, 42%), *GATA3* (7, 37%), *PIK3CA* (5, 26%), *CCND1* (4, 21%), *MAP3K1* (4, 21%), and *NOTCH1* (4, 21%). Among these frequently altered genes, *GATA3* was mainly changed by amplification (6 of 7 patients). Among 50 cancer hallmark genes, the genes most frequently altered by amplification were *ARNT* (11 patients, 58%), *BCL9* (11, 58%), *DDR2* (11, 58%), *FCGR2B* (11, 58%), *LMNA* (11, 57%), and *MYC* (9, 47%) (Supplementary Fig. 2A). We further analyzed the oncogenic pathways affected by somatic mutations. As shown in Fig. 2B, the most frequently altered pathways were the NOTCH pathway (17 patients, 89%), RTK-RAS pathway (15, 79%), WNT pathway (15, 79%), and PI3K pathway (15, 79%). The altered genes in these pathways are shown in Supplementary Figs. 2B–E).

Comparison of genomic alterations between TN-IBC and TN-non-IBC

To identify TN-IBC-specific genomic alterations, we compared the germline and somatic variants between the 19 TN-IBC patients and the 60 stage III and IV TN-non-IBC patients. As shown in Fig. 1C, the number of germline missense variants was significantly lower in TN-IBC than in TN-non-IBC (mean: 63 vs. 277, $p < 0.0001$). However, there were no significant differences between TN-IBC and TN-non-IBC in the numbers of truncating and inframe germline variants. TN-IBC also had a significantly lower somatic mutation load than TN-non-IBC (mean: 96 vs. 236, $p < 0.0001$), including significantly lower loads of missense (mean: 86 vs. 157, $p = 0.0026$), truncating (mean: 9 vs. 58, $p < 0.0001$), and inframe mutations (mean: 2 vs. 21, $p < 0.0001$) (Fig. 2C). Similarly, TN-IBC had significantly lower loads of CNVs than TN-non-IBC (mean: 37 vs. 114, $p < 0.0001$),

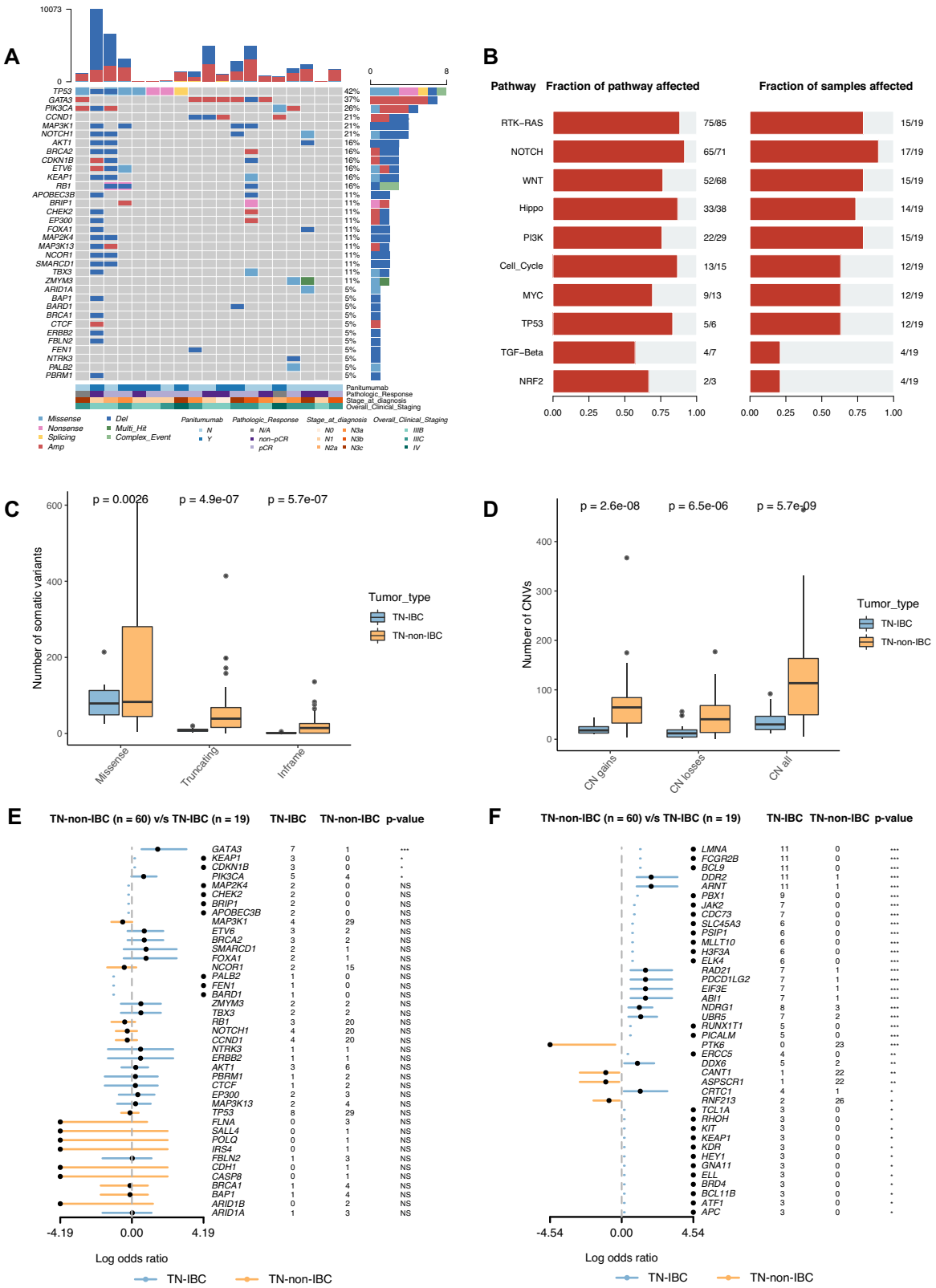

Fig. 2 | Somatic alterations identified in TN-IBC and comparison with TN-non-IBC. A Somatic alterations identified in breast cancer driver genes in TN-IBC. Gene names and relative frequency of mutations are reported in the double y-axis. Top: bar graph defining the total number of different types of somatic alterations in each patient; bottom: annotation for PmAb treatment, pathologic response, stage at diagnosis, and overall clinical staging. **B** Altered oncogenic pathways affected by somatic alterations in TN-IBC. **C**,**D** Number of somatic variants, including missense, truncating, and inframe variants (**C**), and CNV load, including copy number gains, losses, and both (**D**), in TN-IBC and TN-non-IBC. **E**,**F** Enrichment of somatic alterations in breast-cancer-associated genes (**E**) and cancer hallmark genes (**F**) in TN-IBC compared to TN-non-IBC. $^{*}P < 0.05$; $^{**}P < 0.01$; $^{***}P < 0.001$; NS, not significant. In **C** and **D**, the center line represents the median of the data. The edges of the box correspond to the 75th percentile and the 25th percentile respectively, showing the interquartile range (IQR). The whiskers extend to the largest and smallest values within 1.5 times the IQR from the 25th and 75th percentiles. Outliers, defined as data points beyond the whiskers, are plotted individually as dots.

including significantly lower loads of CN gains (mean: 21 vs. 67, $p < 0.0001$) and CN losses (mean: 16 vs. 47, $p < 0.0001$) (Fig. 2D).

Next, we compared the enrichment of somatic genomic alterations between TN-IBC and TN-non-IBC. As shown in Fig. 2E and S3A, TN-IBC had significantly enriched alterations in 4 breast-cancer-associated genes, *GATA3* ($p = 0.0001$, adj-$p = 0.001$), *KEAP1* ($p = 0.01$, adj-$p = 0.05$), *CDKN1B* ($p = 0.01$, adj-$p = 0.05$), and *PIK3CA* ($p = 0.03$, adj-$p = 0.1$), compared to TN-non-IBC. Among these genes, *GATA3* was amplified in 6 of 19 TN-IBC samples but not in TN-non-IBC. As shown in Figs. 2F and S3B, we found that TN-IBC had significantly enriched alterations in 36 cancer hallmark genes, the most significant of which were *LMNA* ($p < 0.0001$, adj-$p < 0.0001$), *FCGR2B* ($p < 0.0001$, adj-$p < 0.0001$), *BCL9* ($p < 0.0001$, adj-$p < 0.0001$), *DDR2* ($p < 0.0001$, adj-$p < 0.0001$), and *ARNT* ($p < 0.0001$, adj-$p < 0.0001$). The majority of the alterations were amplifications. In contrast, TN-non-IBC had enriched alterations in 4 cancer hallmark genes, *PTK6* ($p = 0.0009$, adj-$p = 0.01$), *CANT1* ($p = 0.01$, adj-$p = 0.05$), *ASPSCR1* ($p = 0.01$, adj-$p = 0.05$), and *RNF213* ($p = 0.01$, adj-$p = 0.05$), compared to TN-IBC (Figs. 2F and S2B).

Taken together, our data showed that TN-IBC had a lower germline and somatic mutation burden than TN-non-IBC. We also identified several genes enriched for genomic alterations in TN-IBC compared to TN-non-IBC.

Transcriptomic expression profiles in TN-IBC

To identify genes specifically expressed in patients with TN-IBC, we conducted RNA-seq analyses of the 19 TN-IBC patient samples. The sample-to-sample distance was calculated, and the patient samples were clustered (Fig. 3A). We observed 2 main clusters but did not find any association between the cluster patterns and the clinical characteristics, including clinical stage and pathologic response. Samples in cluster I had a relatively higher TIL percentage than those in cluster II (49% vs. 28%), but the difference was not statistically significant ($p = 0.11$). We further investigated the enriched hallmark pathways in TN-IBC samples. We observed 2 main clusters consistent with the sample similarity clusters (Fig. 3B). Overall, the most enriched pathways across all TN-IBC samples were genes up-regulated associated with angiogenesis (median NES = 0.22), genes in the hedgehog signaling pathway (median NES = 0.20), and genes involved in response to interferon-α proteins (median NES = 0.19). The most enriched pathways in cluster I were the protein secretion pathway (median NES = 0.31) and genes involved in response to interferon-α and -γ (median NES = 0.23). In contrast, the most enriched pathways in cluster II were the Notch signaling pathway (median NES = 0.33) and genes regulated by MYC (median NES = 0.31).

Comparison of gene expression between TN-IBC and TN-non-IBC

To identify genes specifically expressed in TN-IBC, we compared gene expression between the 19 patients with TN-IBC and 19 patients with TN-non-IBC. Sample distance was calculated, and unsupervised hierarchical clustering was performed based on the 5000 most variable genes. Three main clusters were found across groups, including 1 cluster of TN-non-IBC and 2 clusters of TN-IBC (Supplementary Fig. 4A,B). The principal component analysis explained 66% and 5% of the total variance and showed a remarkable separation between TN-IBC and TN-non-IBC (Supplementary Fig. 4C). By conducting differential gene expression analysis, we identified 10,588 differentially expressed genes (absolute Log2FC ≥ 1, adj-$p < 0.05$), among which 4083 genes were significantly upregulated and 6505 genes were significantly down-regulated in TN-IBC relative to TN-non-IBC tumors. The top 50 up-regulated and down-regulated genes in TN-IBC relative to TN-non-IBC tumors are shown in Fig. 3C and Supplementary Fig. 4D. The most up-regulated protein-coding genes in TN-IBC were *PNLIP*, *OR1A2*, *C5orf17*, and *FGA*. The most down-regulated protein-coding genes in TN-IBC were *UBE2Q2P6*, *RGPD5*, *NSFP1*, *RGPD1*, *RP11-645C24.2*, and *RPS17L*. Strikingly, we observed up-regulation of many microRNAs (miRNAs) in TN-IBC (Supplementary Fig. 4D).

We further compared the expression of breast-cancer-associated genes in TN-IBC and TN-non-IBC. As shown in Fig. 3D, 15 breast-cancer-associated genes were significantly overexpressed in TN-IBC compared to TN-non-IBC, including *BRCA1* (Log2FC = 2.02, adj-$p < 0.0001$), *BRCA2* (Log2FC = 2.21, adj-$p < 0.0001$), *PIK3CA* (Log2FC = 1.73, adj-p < 0.0001), *PALB2* (Log2FC = 1.85, adj-$p < 0.0001$), and *RB1* (Log2FC = 1.11, adj-$p < 0.0001$). The expression of 9 breast-cancer-associated genes was significantly downregulated in TN-IBC compared to TN-non-IBC, including *TP53* (Log2FC = -1.06, adj-$p = 0.005$), *CHEK2* (Log2FC = -2.45, adj-$p < 0.0001$), *CDKN1B* (Log2FC = -1.46, adj-$p < 0.0001$), *NOTCH1* (Log2FC = -1.31, adj-$p < 0.0001$), and *CCND1* (Log2FC = -1.31, adj-$p = 0.004$). We also performed GSEA to evaluate the pathways differentially enriched between TN-IBC and TN-non-IBC. As shown in Figs. 3E, 4 hallmark gene sets were significantly enriched in TN-IBC, including mitotic spindle (NES = 2.18, adj-$p < 0.0001$), protein secretion (NES = 1.87, adj-$p = 0.0005$), UV response (NES = 1.84, adj-p < 0.0001), and spermatogenesis (NES = 1.55, adj-$p = 0.01$). Only 1 hallmark gene set, MYC targets V1, was significantly enriched in TN-non-IBC (NES = -1.74, adj-$p < 0.0001$).

Taken together, our data identified several genes with significantly higher expression in TN-IBC than in TN-non-IBC. Further studies are needed to determine whether these genes specifically contribute to the aggressiveness and the distinctive biology of TN-IBC.

Estimation of immune cell fractions in TN-IBC and TN-non-IBC by deconvolution analysis

It has been reported that the TME is a driving force of IBC aggressiveness. To understand the immune microenvironment of TN-IBC tumors, we deconvoluted 22 types of immune cells from the RNA-seq data of TN-IBC. Supplementary Fig. 4E shows the relative percentages of immune cells in each TN-IBC patient. The most abundant immune cells were M2 macrophages, resting $CD4^+$ memory T cells, and M1 macrophages. Next, we examined whether TN-IBC and TN-non-IBC have distinct immune landscapes. We deconvoluted 22 types of immune cells from the RNA-seq data of 19 TN-non-IBC patient samples and compared the percentages of different immune cells to those in the TN-IBC patient samples. As shown in Fig. 3F, TN-IBC had significantly higher relative fractions of gamma-delta (γδ) T cells ($p = 0.004$), M1 macrophages ($p = 0.01$), and eosinophils ($p = 0.02$) than TN-non-IBC. In contrast, TN-non-IBC had significantly higher relative fractions of CD8 T cells ($p = 0.01$) and resting dendritic cells ($p = 0.01$) than TN-IBC. These results suggest that the TN-IBC immune microenvironment is more immunosuppressive than the TN-non-IBC immune microenvironment.

Comparison of genomic alterations between pCR and non-pCR groups in TN-IBC

As shown in Supplementary Fig. 1, TN-IBC samples analyzed in this study were collected from a randomized phase II trial (NCT02876107). Data on pCR were available for 10 patients in the NAC arm, including 6 with pCR and 4 with non-pCR, and 7 patients in the PmAb/NAC arm, including 4 with pCR and 3 with non-pCR. To understand the relationship of genomic alterations to treatment response, we assessed the associations of somatic mutation load and CNV load with pCR status in the NAC and PmAb/NAC arms, respectively. As shown in Fig. 4A, in the NAC arm, patients who achieved a pCR had a significantly higher mutation load than those who did not (mean: 119 vs. 58, $p = 0.04$). In the PmAb/NAC arm, the mean mutation load was higher in the patients who achieved a pCR than in those who did not, but the difference was not statistically significant (mean: 111 vs. 76, $p = 1$). CNV load did not differ between the pCR and non-pCR groups in either the NAC arm or the PmAb/NAC arm (Fig. 4B).

We further analyzed the alterations of breast-cancer-associated genes in each arm. The most frequently altered gene in the NAC arm was *GATA3* (4 patients, 40%) (Figs. 4C and S5A), and the most frequently altered gene in the PmAb/NAC arm was *TP53* (5 patients, 71%) (Figs. 4D and S5B). We

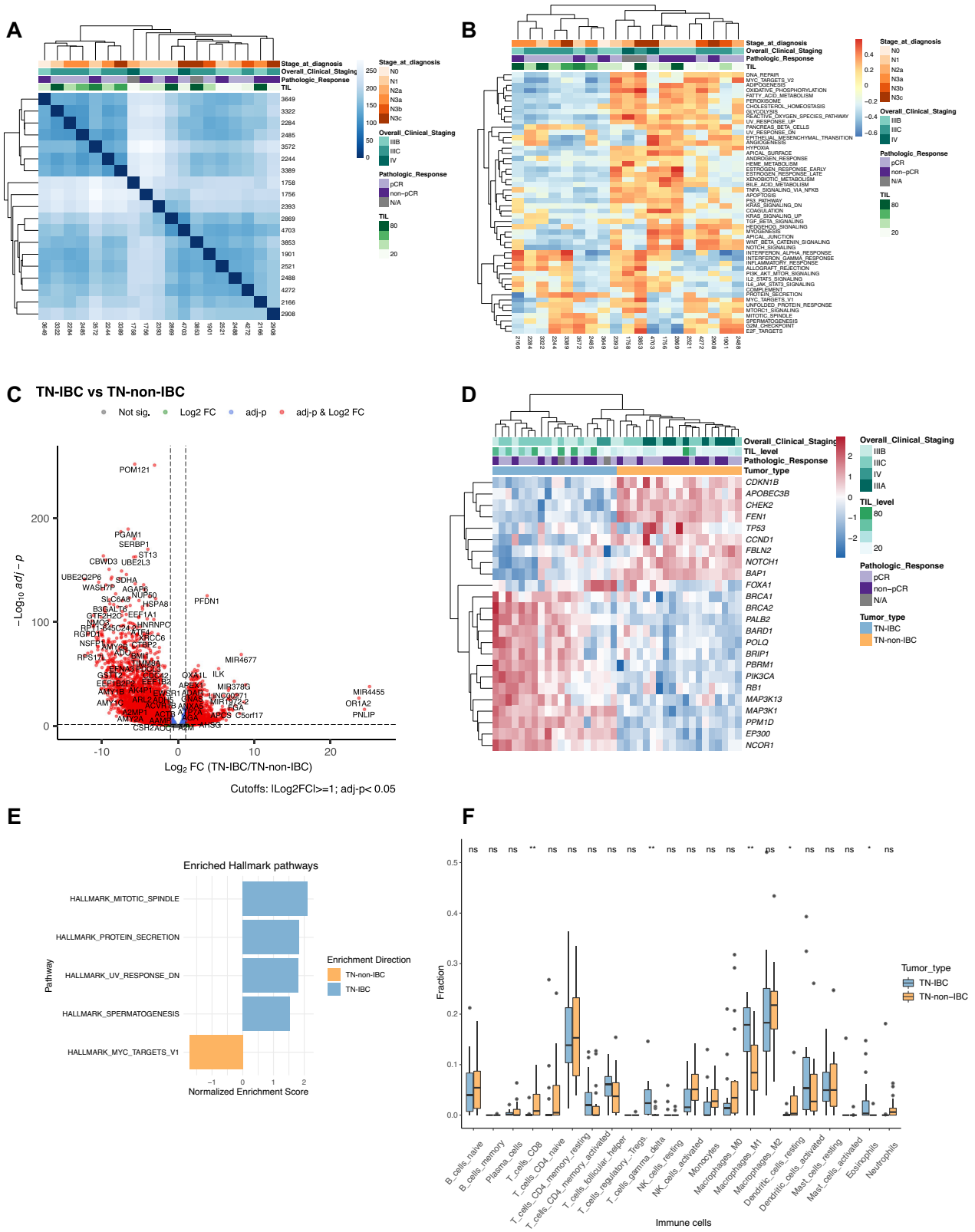

Fig. 3 | Transcriptomic profiles of TN-IBC and comparison with TN-non-IBC. **A** Heatmap of sample-to-sample distances calculated from the RNA expression profiles of TN-IBC. **B** Heatmap of the enrichment scores of cancer hallmark pathways in TN-IBC. **C** Volcano plot of differentially expressed genes with Log2FC ≥ 1 or ≤−1 and adj-p < 0.05 in TN-IBC compared to TN-non-IBC. **D** Heatmap of the differentially expressed breast-cancer-associated genes in TN-IBC compared to TN-non-IBC. **E** GSEA of the significantly enriched hallmark pathways in TN-IBC compared to TN-non-IBC. **F** Relative immune cell fractions in TN-IBC and TN-non-IBC analyzed by CIBERSORT. *P < 0.05; **P < 0.01; NS, not significant. In **A**,**B**,**D** Top: annotation for stage at diagnosis, overall clinical stage, pathologic response, and TIL. In **F**, the center line represents the median of the data. The edges of the box correspond to the 75th percentile and the 25th percentile respectively, showing the interquartile range (IQR). The whiskers extend to the largest and smallest values within 1.5 times the IQR from the 25th and 75th percentiles. Outliers, defined as data points beyond the whiskers, are plotted individually as dots.

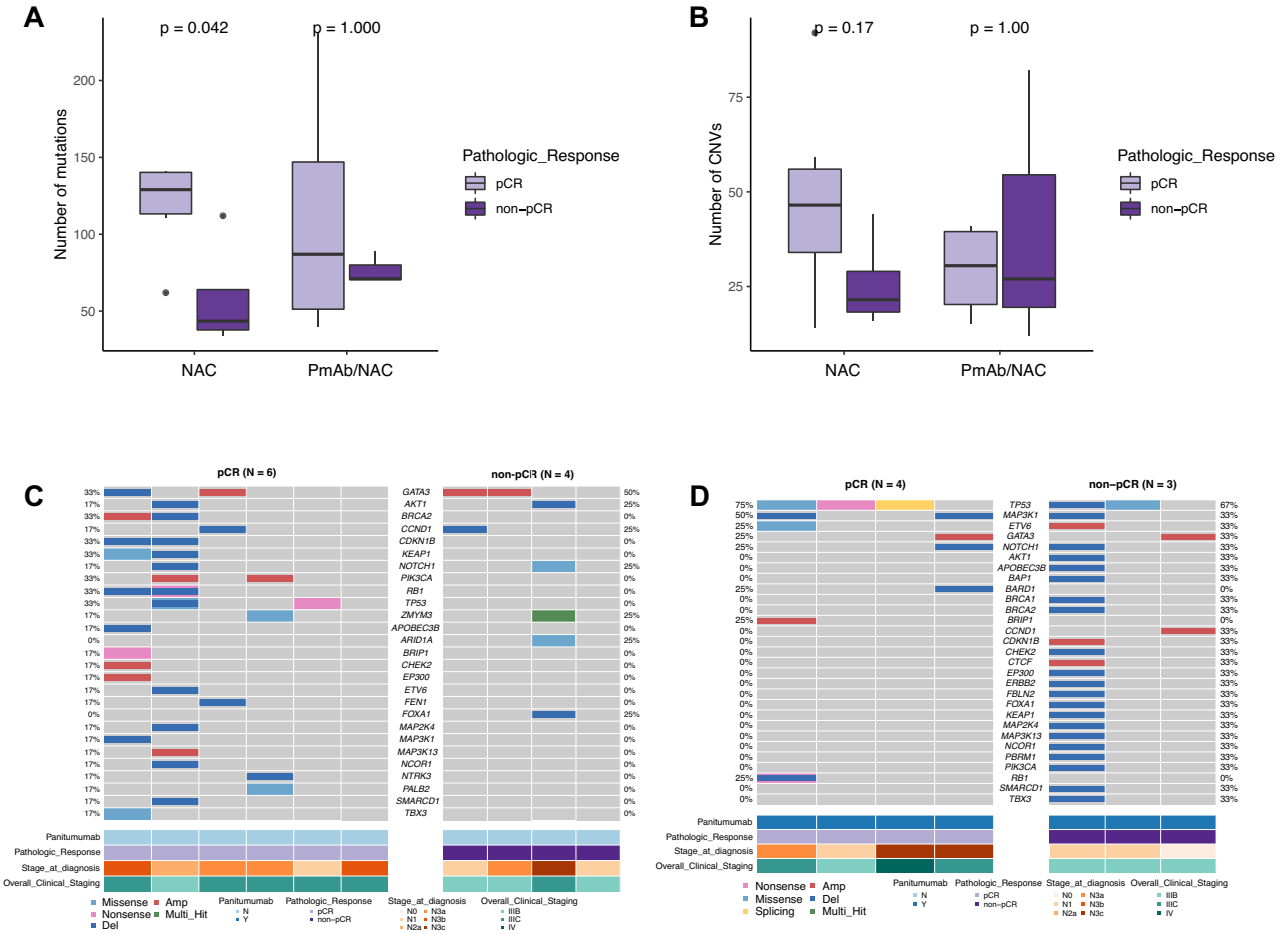

Fig. 4 | Comparison of somatic alterations between tumor samples collected from TN-IBC patients who did and did not have pCRs in the NAC and PmAb/NAC arms. A,**B** Comparison of somatic mutation load (**A**) and CNV load (**B**) between TN-IBC patients who did and did not have pCRs in the NAC and PmAb/NAC arms. **C**,**D** Somatic alterations of breast-cancer-associated genes identified in tumor samples from TN-IBC patients who did and did not have pCRs in the NAC (**C**) and PmAb/NAC arms (**D**). Gene names and relative frequency of mutations are reported in the double y-axis. Bottom: annotation for PmAb treatment, pathologic response, stage at diagnosis, and overall clinical stage. In **A** and **B**, the center line represents the median of the data. The edges of the box correspond to the 75th percentile and the 25th percentile respectively, showing the interquartile range (IQR). The whiskers extend to the largest and smallest values within 1.5 times the IQR from the 25th and 75th percentiles. Outliers, defined as data points beyond the whiskers, are plotted individually as dots.

also compared the genomic alterations between the pCR and non-pCR groups in each arm. However, we did not find any statistically significant differences likely due to the small sample size. These results suggest that patients with higher mutation load achieved better responses to NAC. The association of genomic alterations with response to PmAb/NAC needs to be further studied in a larger sample size.

As shown in Supplementary Fig. 5C, in the analysis comparing the 6 patients with a pCR in the NAC group with all 7 patients with a non-PCR in both groups, the somatic mutation load in the pCR group was significantly higher than that in the non-pCR group (mean: 119 vs. 66, $p = 0.03$). There was also a trend toward a higher CNV load in the pCR group, as well as trends towards higher loads of CN gains and CN losses. However, the differences were not statistically significant (Supplementary Fig. 5D). We further compared the enrichment of genomic alterations in the pCR and non-pCR groups but did not find any significant enrichment of genes or oncogenic pathways in either group (Supplementary Fig. 5E).

Comparison of gene expression and enriched pathways between pCR and non-pCR groups in TN-IBC

Next, we compared gene expression between the pCR and non-pCR groups of TN-IBC patients in the NAC and PmAb/NAC arms. In the NAC arm, a total of 112 differentially expressed genes were identified with an adj-$p < 0.05$ and absolute Log2FC ≥ 1, including 63 genes up-regulated in the pCR group and 49 genes up-regulated in the non-pCR group (Figs. 5A and S6A). The most up-regulated genes in the pCR group relative to non-pCR group were *KRT36* (Log2FC = 23.07, adj-$p < 0.0001$), *KRT43P* (Log2FC = 22.58, adj-$p < 0.0001$), and *OR6K3* (Log2FC = 22.04, adj-$p < 0.0001$) (Figs. 5A and S6B). The most down-regulated genes in the pCR group relative to non-pCR group were *ANKRD1* (Log2FC = −5.67, adj-$p = 0.0004$), *ADH1C* (Log2FC = −5.16, adj-$p = 0.001$), and *SERPINA11* (Log2FC = −3.96, adj-$p = 0.03$) (Figs. 5A and S6B). GSEA showed 4 pathways enriched in the pCR group (Fig. 5C), including pancreas beta cells (NES = 1.89, adj-$p = 0.007$), MTORC1 signaling (NES = 1.76, adj-$p < 0.0001$), E2F targets (NES = 1.71, adj-$p = 0.0002$), and spermatogenesis (NES = 1.50, adj-$p = 0.02$). Eleven pathways were significantly enriched in the non-pCR group, and the most significant ones were estrogen response early (NES = −2.27, adj-$p < 0.0001$), myogenesis (NES = −1.98, adj-$p < 0.0001$), and p53 pathway (NES = −1.88, adj-$p < 0.0001$).

In the PmAb/NAC arm, 76 differentially expressed genes were identified with an adj-p < 0.05 and absolute Log2FC ≥ 1, including 24 genes up-regulated in the pCR group and 52 genes up-regulated in the non-pCR group (Figs. 5B and S6C). The most up-regulated genes in the pCR group were *SERPINA9* (Log2FC = 22.09, adj-$p < 0.0001$), *OR52N5* (Log2FC = 7.96, adj-$p = 0.01$), and *CLEC3A* (Log2FC = 7.52, adj-$p = 0.008$) (Figs. 5B

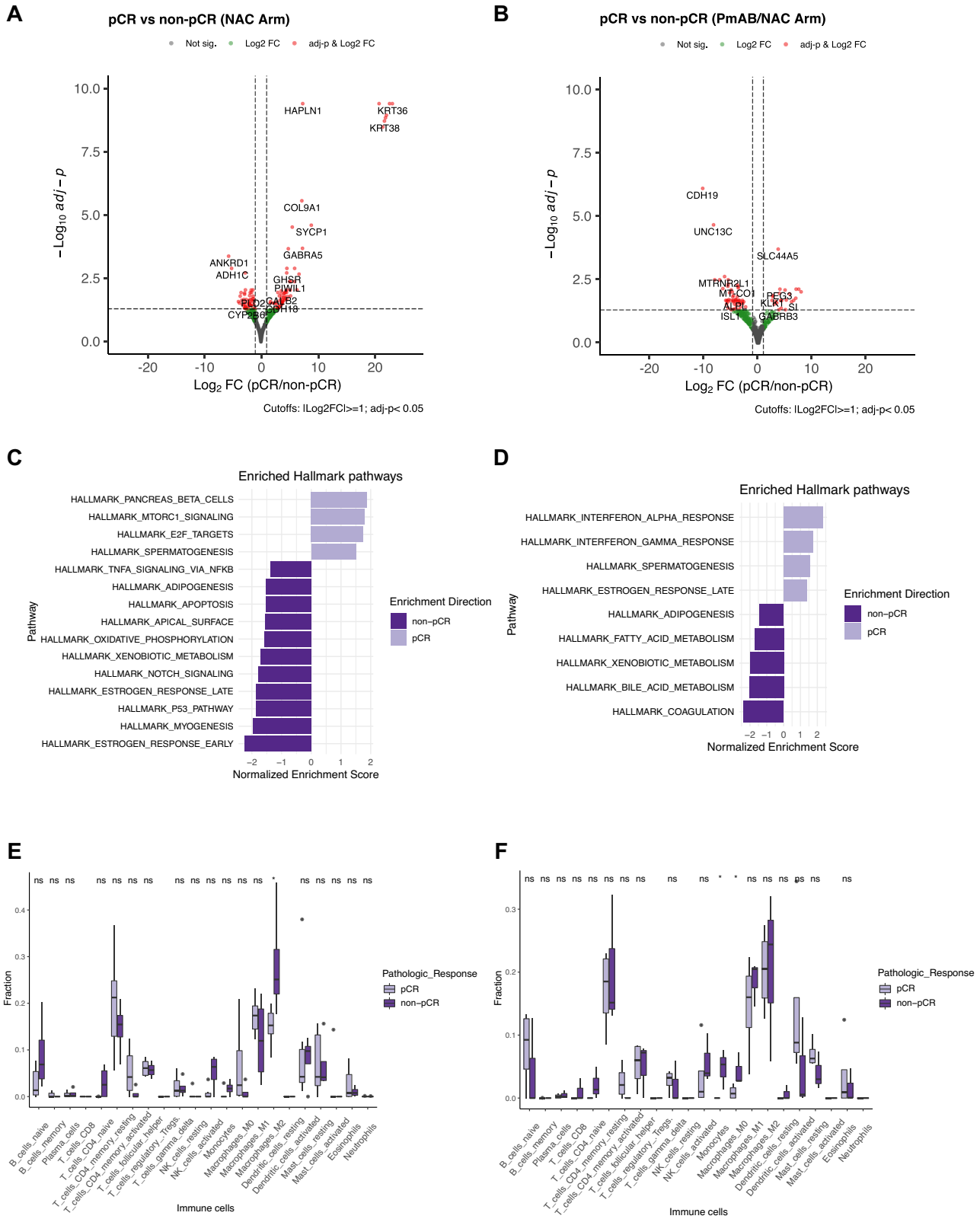

Fig. 5 | Comparison of gene expression and immune cell composition between tumor samples collected from TN-IBC patients who did and did not have pCRs in the NAC and PmAb/NAC arms. A,**B** Volcano plots of differentially expressed genes with Log2FC ≥ 1 or ≤−1 and adj-p < 0.05 in tumor samples collected from TN-IBC patients who did and did not have pCRs in the NAC (**A**) and PmAb/NAC (**B**) arms. **C**,**D** GSEA of the significantly enriched hallmark pathways in tumor samples collected from TN-IBC patients who did and did not have pCRs in the NAC (**C**) and PmAb/NAC (**D**) arms. **E**,**F** Comparison of the immune cell composition in tumor samples collected from TN-IBC patients who did and did not have pCRs in the NAC (**E**) and PmAb/NAC (**F**) arms. *P < 0.05; NS, not significant. In **E** and **F**, the center line represents the median of the data. The edges of the box correspond to the 75th percentile and the 25th percentile respectively, showing the interquartile range (IQR). The whiskers extend to the largest and smallest values within 1.5 times the IQR from the 25th and 75th percentiles. Outliers, defined as data points beyond the whiskers, are plotted individually as dots.

and S6D). The most up-regulated genes in the non-pCR group were *CDH19* (Log2FC = −10.22, adj-p < 0.0001), *UNC13C* (Log2FC = −8.22, adj-p < 0.0001), and *VWC2* (Log2FC = −8.0, adj-p = 0.003) (Figs. 5B and S6D). GSEA showed 4 pathways enriched in the pCR group (Fig. 5D), including interferon-alpha response (NES = 2.37, adj-p < 0.0001), interferon-γ response (NES = 1.79, adj-p < 0.0001), spermatogenesis (NES = 1.60, adj-p = 0.02), and estrogen response late (NES = 1.40, adj-p = 0.02). Five pathways were significantly enriched in the non-pCR group, including coagulation (NES = −2.43, adj-p < 0.0001), bile acid metabolism (NES = −2.05, adj-p < 0.0001), xenobiotic metabolism (NES = −2.0, adj-p < 0.0001), fatty acid metabolism (NES = −1.75, adj-p = 0.001), and adipogenesis (NES = −1.42, adj-p = 0.04).

We also compared gene expression between the pCR group in the NAC arm (N = 6) and the non-pCR groups in both the NAC and PmAb/NAC arms (N = 7). A total of 133 differentially expressed genes were identified (Supplementary Fig. 7A,B). Among these, 41 genes were up-regulated in the pCR group, and 92 genes were up-regulated in the non-pCR group (Supplementary Fig. 7B). The most up-regulated genes in the pCR group were *COL9A1* (Log2FC = 22.59, adj-p < 0.0001), *OR10K2* (Log2FC = 21.47, adj-p < 0.0001), and *TPD52L3* (Log2FC = 7.53, adj-p < 0.0001) (Supplementary Fig. 7C). The most up-regulated genes in the non-pCR group were *GPR15LG* (Log2FC = −22.54, adj-p < 0.0001), *UGT2B15* (Log2FC = −6.23, adj-p = 0.003), and *DDX3Y* (Log2FC = −5.54, adj-p = 0.001) (Supplementary Fig. 7C). The GSEA results are shown in Supplementary Fig. 7D. Four hallmark gene sets were significantly enriched in the pCR group, including pancreas beta cells (NES = 2.03, adj-p = 0.0008), spermatogenesis (NES = 2.04, adj-p < 0.0001), E2F targets (NES = 1.90, adj-p < 0.0001), and G2M checkpoint (NES = 1.63, adj-p = 0.0007). Fourteen gene sets were significantly enriched in the non-pCR group, including estrogen response early (NES = −2.24, adj-p < 0.0001), myogenesis (NES = −2.0, adj-p < 0.0001), xenobiotic metabolism (NES = −1.89, adj-p < 0.0001), p53 pathway (NES = −1.88, adj-p < 0.0001), and adipogenesis (NES = −1.47, adj-p < 0.0001).

In summary, we identified differentially expressed genes between TN-IBC patients who achieved a pCR and who did not achieve a pCR to NAC or PmAb/NAC. These genes may be candidates that can be targeted to enhance the response of TN-IBC to NAC or PmAb/NAC.

Comparison of immune cell composition between pCR and non-pCR groups in TN-IBC

We further compared the immune cell composition between the pCR and non-pCR groups of TN-IBC patients in the NAC and PmAb/NAC arms using deconvolution analysis (Supplementary Fig. 8A). In the NAC arm, the percentage of M2 macrophages was significantly higher in the non-pCR group (p = 0.038) (Fig. 5E). In the PmAb/NAC arm, the percentages of monocytes (p = 0.032) and M0 macrophages (p = 0.05) were significantly higher in the non-pCR group (Fig. 5F). These results suggest that the presence of immunosuppressive macrophages in the tumor may contribute to the worse response of TN-IBC to NAC or PmAb/NAC.

As the sample sizes of the NAC and PmAb/NAC arms were small, we combined the data from the 2 arms and compared the immune cell composition between the pCR and non-pCR groups. As shown in Supplementary Fig. 8B, the percentage of activated memory $CD4^+$ T cells was significantly higher in the pCR group (p = 0.02). In contrast, the percentages of activated NK cells (p = 0.02) and monocytes (p = 0.04) were significantly higher in the non-pCR group.

Taken together, our data indicated that TN-IBC and TN-non-IBC have distinct TMEs, and the presence of more immunosuppressive macrophages may be associated with the worse response of TN-IBC to NAC or PmAb/NAC. These results suggest that targeting macrophages may improve the treatment of patients with TN-IBC.

Discussion

To our knowledge, our present work is the first multi-omics characterization of clinically annotated TN-IBC specimens and the first comprehensive comparison of TN-IBC specimens with stage III TN-non-IBC specimens selected on the basis of patient stage and sequencing protocol and platform. We identified germline and somatic alterations and transcriptomic and immunological features that distinguish TN-IBC from TN-non-IBC. Further, we identified genomic and transcriptomic features that may be associated with the pathological response of TN-IBC to NAC and PmAb/NAC, the treatment regimen with the historically highest pCR in patients with TN-IBC.

The distinctive features of TN-IBC revealed by our study include the lower baseline tumor mutation load and CNV load and the association of immunosuppressive tumor-infiltrating immune components with an unfavorable response to NAC. Previous studies have shown higher tumor mutational burden in IBC than in non-IBC with mixed subtypes or HER2-positive subtype[10,15,47]. One study involving targeted next-generation sequencing of 91 "breast cancer-specific" genes in 156 cases of IBC, including 51 cases of TN-IBC, and 197 invasive breast carcinomas from the TCGA, the non-IBC dataset, showed that gene mutation frequencies were not significantly different in the TN-IBC and TN-non-IBC subgroups. In our study, we compared the genomic alterations of TN-IBC samples to those of TN-non-IBC samples that were sequenced using the same protocol and platform. We showed that TN-IBC had a significantly lower number of germline missense variants; lower somatic mutation load, including missense, truncating, and inframe mutations; and lower loads of copy number gains and losses. This is the first report of lower mutation load in TN-IBC compared to TN-non-IBC. It has been reported that tumors with higher mutation load express more mutation-associated neoantigens that can be recognized by the immune system, and tumors with lower mutation load could be less likely to trigger a robust immune response[48,49]. Indeed, we observed a lower fraction of CD8 T cells in TN-IBC samples than in TN-non-IBC samples as revealed by deconvolution analysis, indicating the "cold" immune microenvironment in TN-IBC tumors. Consistent with this finding, we observed that TN-IBC patients who achieved a pCR to NAC had a significantly higher mutation load than those who did not. Patients who achieved a pCR to NAC also had lower fractions of immunosuppressive M2 macrophages compared to patients who did not achieve a pCR to NAC. These results support the potential connection between lower mutation loads and a weaker antitumor immune response. It is important to note that factors such as sample size, patient selection, and technical differences in sequencing methods used in other studies may have collectively influenced the observed mutational burden, leading to the discrepancy. In our study, we sequenced all patients using the same protocol and platform and processed the data with a consistent bioinformatics pipeline to minimize variability.

One of the significant findings of our study is the identification of higher fractions of M1 macrophages, γδ T cells, and eosinophils in TN-IBC than TN-non-IBC. The enriched M1 macrophages and γδ T cells in TN-IBC are consistent with the deconvolution analysis data reported by Bertucci et al.[50]. However, their data showed more immune differences between hormone-receptor-positive, HER2-negative IBC and non-IBC than between TN-IBC and TN-non-IBC[50]. γδ T cells are T cells that have a γδ T-cell receptor on the surface, participate in various immune responses, and have functions in both promoting and inhibiting antitumor responses. Eosinophils are a variety of white blood cells and one of the immune components combating multicellular parasites and certain infections[51]. There is conflicting evidence suggesting that eosinophils in the TME have antitumor activities[52–54] and tumor-promoting effects[55,56]. In a TGIRT-seq study to identify IBC distinctive genes (unpublished data), we also observed a higher fraction of eosinophils in TN-IBC tumor tissues than in TN-non-IBC tumor tissues. The role of γδ T cells and eosinophils in the progression of IBC is worth further investigation.

Our study also demonstrated the potential role of the TME in mediating response of TN-IBC to NAC or PmAb/NAC. In both the NAC and PmAb/NAC arms, patients with a non-pCR had higher fractions of immunosuppressive macrophages, suggesting that macrophages are a potential target to improve the therapeutic efficacy of NAC or PmAb/NAC for TN-IBC patients. The enriched interferon-α and -γ response in the group with a pCR to PmAb/NAC and the higher fraction of immunosuppressive macrophages

in the groups with a non-pCR to NAC and PmAb/NAC suggest that an immunoactive TME is the key to better response to NAC or PmAb/NAC. This is consistent with our recent finding that a pCR to PmAb/NAC in patients with IBC may be associated with an immunoactive TME induced by PmAb, including an increase in $CD8^+$ T cells and a decrease in regulatory T cells and M2 macrophages after PmAb treatment[57]. We can potentially reprogram the tumor-associated macrophages to a tumoricidal phenotype, inhibiting their recruitment to the tumor site. Understanding the specific roles and mechanisms of macrophages in TN-IBC will be crucial for developing effective macrophage-targeted interventions.

Our study identified several novel genomic alterations in TN-IBC. The 12 most frequently altered genes in TN-IBC were *ARNT*, *BCL9*, *DDR2*, *FCGR2B*, *LMNA*, *MYC*, *TP53*, *GATA3*, *PIK3CA*, *CCND1*, *MAP3K1*, and *NOTCH1*. The somatic alterations of *MYC*, *TP53*, *GATA3*, *PIK3CA*, *CCND1*, and *NOTCH1* in TN-IBC are consistent with previous reports in IBC with all subtypes[47]. However, only *GATA3*, *PIK3CA*, *ARNT*, *DDR2*, *BCL9*, *FCGR2B*, and *LMNA* had significantly enriched alterations in TN-IBC compared to TN-non-IBC (Fig. 2E,F). Among these genes, *ARNT*, *DDR2*, *BCL9*, *FCGR2B*, and *LMNA* in TN-IBC were identified for the first time (Fig. 2F). *ARNT*, also designated as hypoxia-inducible factor-1β, encodes a protein that promotes the expression of genes involved in xenobiotic metabolism and functions as a co-factor for transcriptional regulation by hypoxia-inducible factor 1[58]. ARNT is especially required during early stages of tumor growth[58]. DDR2 is a receptor tyrosine kinase that regulates collagen-cell interactions[59]. The overexpression, amplification, and mutations of DDR2 can drive aggressive phenotype of several types of cancer[60,61]. BCL9 plays a critical role in the progression of colorectal cancer, multiple myeloma, and ductal carcinoma in situ by activating Wnt signaling[62,63]. FCGR2B can inhibit the functions of activating FcγRs, such as phagocytosis and proinflammatory cytokine release[64]. It also has a negative regulatory role in BCR-induced or CD40- and IL-4-mediated B-cell activation[65]. LMNA plays an important role in maintaining genome integrity. Altered LMNA levels can impact the ability of cells to repair DNA damage, potentially accelerating mutagenesis and promoting tumor initiation and progression[66]. How amplification alterations of these genes affect the tumorigenesis and progression of TN-IBC needs to be further investigated.

Alterations of *GATA3* and *PIK3CA* in IBC have been reported previously[47]. *GATA3* belongs to the GATA family of transcription factors and is one of the most frequently mutated genes in breast cancer, which is an essential regulator of T-cell development[67–69]. The present study showed that 37% of TN-IBC samples had *GATA3* copy gains and *GATA3* deletion mutation, mostly amplification (6 of the 7 TN-IBC samples with *GATA3* alterations). Although *GATA3* alterations were significantly enriched in TN-IBC compared to TN-non-IBC, we did not observe significant differences in the expression of *GATA3* between TN-IBC and TN-non-IBC on RNA-seq analysis. It has been reported that *GATA3* copy number gains are more frequently found in invasion-prone breast tumors and this pattern is likely due to epigenetic regulations[70]. It is possible that *GATA3* alterations affect IBC progression via epigenetic regulation instead of gene expression regulation, which needs to be further investigated. Alterations in the PI3K pathway are among the most frequent oncogenic aberrations in TNBC[71]. *PIK3CA* is an oncogene in the PI3K pathway and is the second most frequently mutated gene in TNBC, following *TP53*. In the TN-IBC cohort in our present study, 22 of 29 fractions of PI3K pathway were affected, 15 of 19 patients had PI3K pathway alterations (Fig. 2B), and *PIK3CA* was mutated in 5 of 19 patients (26%), mirroring previously reported data for metastatic IBC[13] and TN-IBC[14]. *PIK3CA* mutations identified in our study included amplifications, deletions, and missense mutations in 3, 1, and 1 of the 5 TN-IBC patients with *PIK3CA* alterations, respectively. We also showed that *PIK3CA* gene expression in TN-IBC was 3.3-fold higher than that in TN-non-IBC (adj-p = 3.72E-11). *PIK3CA* mutation has been reported to confer resistance to chemotherapy in TNBC by inhibiting apoptosis and activating the PI3K/AKT/mTOR signaling pathway[72]. Given that *PIK3CA* mutations and gene expression were enriched in TN-IBC compared to TN-non-IBC, *PIK3CA* may represent a unique targetable oncogene for TN-IBC. Specific inhibitors of PI3K, such as Apelisib, have shown efficacy in PIK3CA-mutant cancers. Given the enrichment of PIK3CA mutations in TN-IBC, these inhibitors could be useful for this aggressive cancer type. Additionally, combining PI3K inhibitors with treatments such as chemotherapy, immunotherapy, or other targeted therapies might improve outcomes for TN-IBC patients with PIK3CA alterations. Further research is needed to fully understand the potential of targeting PIK3CA in TN-IBC. Understanding the molecular mechanisms driving PIK3CA-related cancer in TN-IBC will also help identify biomarkers for treatment response and resistance, leading to more precise and effective therapies.

In addition to the genomic alterations and immunological features that distinguish TN-IBC tumors from TN-non-IBC tumors, we identified several transcriptomic characteristics of TN-IBC that may function as potential drivers of TN-IBC aggressiveness and serve as prognostic markers for TN-IBC. Among the up-regulated protein-coding genes in TN-IBC, *FGA*, *FGB*, and *FGG* encode the α, β, and γ polypeptide chains of fibrinogen, respectively. Fibrinogen is an extracellular matrix protein involved in the formation of blood clots and is a key biological factor involved in tumor angiogenesis, development[73], and a series of inflammatory diseases possibly mediated by cell-specific integrin and non-integrin receptors on different cell types, including cancer cells, macrophages, monocytes, mast cells, and vascular endothelial cells[74,75]. The blood level of fibrinogen rises in response to systemic inflammation and is elevated in various cancers. It has been reported that plasma fibrinogen level is a potential predictive biomarker of response to neoadjuvant chemotherapy for breast cancer[76,77]. Studies showed that FGG can promote the migration and invasion of hepatocellular cancer cells by activating epithelial to mesenchymal transition[78]. The high expression of genes encoding fibrinogen chains revealed in our study suggests that fibrinogen and 3 chains composed of fibrinogen may contribute to tumorigenesis and progression of TN-IBC, which needs to be further studied. It is also worth investigating whether plasma fibrinogen could be a prognostic or predictive biomarker for TN-IBC. In addition, we observed up-regulation of miRNAs in TN-IBC compared to TN-non-IBC. Among the top 60 up-regulated genes with Log2FC > 5, adj-p < 0.00001, the majority were miRNAs (Supplementary Fig. 4D). miRNAs play critical roles in breast cancer cell proliferation, metastasis, angiogenesis, migration, and survival. Van der Auwera et al. identified 13 miRNAs whose expression differed between IBC and non-IBC[79]. In our study, we also identified significant up-regulation of miRNAs in TN-IBC. However, the function of most of these miRNAs in breast cancer and IBC is largely unknown and needs to be further investigated.

PmAb/NAC has produced the highest pCR rate achieved in patients with TN-IBC[80]. Identifying predictive biomarkers is critical to select patients for this treatment regimen. Our study is the first attempt to identify the association of genetic, transcriptomic, and immunological characteristics of TN-IBC patients with the pCR outcome of NAC or PmAb/NAC. For NAC, TN-IBC patients who achieved a pCR had a significantly higher mutation load, up-regulated expression of *KRT36*, *KRT43P*, and *OR6K3*, and enriched MTORC1 signaling and E2F targets compared to patients who did not achieve a pCR. Although the small sample size limits the identification of genetic alterations associated with a pCR to PmAb/NAC, we identified the up-regulation of *SERPINA9*, *OR52N5*, and *CLEC3A* gene expression and enriched interferon-α and -γ response in the pCR group. In addition, non-pCR patients in both the NAC and PmAb/NAC arms had higher fractions of immunosuppressive macrophages, suggesting that macrophages are a potential target to improve the therapeutic efficacy of NAC or PmAb/NAC for TN-IBC patients.

Our study has several limitations. First, the small sample size limits the analysis. IBC is a sporadic disease without know risk factors, and the overall incidence of IBC from 1973 to 2015 was 2.76 cases per 100,000 people[2]. Among IBC cases, only approximately 20% to 40% are TN-IBC[81]. In addition, IBC tumors are dispersed and do not always form a mass, making it difficult to obtain high-quality core biopsy specimens for sequencing, which limited the number of baseline core biopsy specimens collected in this trial. Second, we compared TN-IBC WES and RNA-seq data to those of stage III TN-non-IBC patient samples from the MD Anderson Cancer Center Moon Shots Program to identify TN-IBC-distinctive genomic and

transcriptomic features. However, the Moon Shots Program did not conduct multiplexed immunofluorescence staining for TN-non-IBC patient samples. This limits the validation of findings from deconvolution analysis and the identification of other novel immune components that are differentially expressed in TN-IBC patients. MD Anderson Cancer Center has opened a prospective trial to profile more patients with rare tumors, including IBC, which may lead to future sequencing and immune profiling of more IBC tumors. Third, the comparison of genomic changes under neoadjuvant systemic therapy is underpowered; these data should be considered hypothesis-generating at this stage.

In summary, here we present an in-depth molecular characterization of clinically annotated primary TN-IBC, a comprehensive comparison of TN-IBC with stage III TN-non-IBC, and comparisons between pCR and non-pCR groups in TN-IBC patients. Our study has identified significant differences in genomic alterations, gene expression, pathway enrichment, and immune cell levels between TN-IBC and TN-non-IBC. Our findings have the potential to elucidate the etiology of TN-IBC and advance the discovery of novel prognostic biomarkers.

Data availability

The WES and RNA-seq data from this study have been deposited in the European Genome-Phenome Archive (Study accession ID: EGAS00001007520; WES accession ID: EGAD00001011648; RNA-seq accession ID: EGAD00001011649).

Received: 4 May 2024; Accepted: 1 October 2024;
Published online: 18 November 2024

References

1. Cristofanilli, M., Buzdar, A. U. & Hortobagyi, G. N. Update on the management of inflammatory breast cancer. *Oncologist* **8**, 141–148 (2003).
2. Abraham, H. G., Xia, Y., Mukherjee, B. & Merajver, S. D. Incidence and survival of inflammatory breast cancer between 1973 and 2015 in the SEER database. *Breast Cancer Res Treat.* **185**, 229–238 (2021).
3. Dawood, S. et al. Differences in survival among women with stage III inflammatory and noninflammatory locally advanced breast cancer appear early: a large population-based study. *Cancer* **117**, 1819–1826 (2011).
4. Yamauchi, H. et al. Inflammatory breast cancer: what we know and what we need to learn. *Oncologist* **17**, 891–899 (2012).
5. Masuda, H. et al. Long-term treatment efficacy in primary inflammatory breast cancer by hormonal receptor- and HER2-defined subtypes. *Ann. Oncol.* **25**, 384–391 (2014).
6. Schmid, P. et al. Keynote-522 Investigators. Pembrolizumab for early triple-negative breast cancer. *N. Engl. J. Med.* **382**, 810–821 (2020).
7. Luo, R. et al. Whole-exome sequencing identifies somatic mutations and intratumor heterogeneity in inflammatory breast cancer. *NPJ Breast Cancer* **7**, 72 (2021).
8. Li, X. et al. Whole-genome sequencing of phenotypically distinct inflammatory breast cancers reveals similar genomic alterations to non-inflammatory breast cancers. *Genome Med.* **13**, 70 (2021).
9. Bertucci, F. et al. Gene expression profiling for molecular characterization of inflammatory breast cancer and prediction of response to chemotherapy. *Cancer Res.* **64**, 8558–8565 (2004).
10. Goh, G. et al. Clonal evolutionary analysis during HER2 blockade in HER2-positive inflammatory breast cancer A phase II open-label clinical trial of Afatinib +/- Vinorelbine. *PLoS Med.* **13**, e1002136 (2016).
11. Hamm, C. A. et al. Genomic and immunological tumor profiling identifies targetable pathways and extensive CD8+/PDL1+ immune infiltration in inflammatory breast cancer tumors. *Mol. Cancer Ther.* **15**, 1746–1756 (2016).
12. Liang, X. et al. Targeted next-generation sequencing identifies clinically relevant somatic mutations in a large cohort of inflammatory breast cancer. *Breast Cancer Res.* **20**, 88 (2018).
13. Matsuda, N. et al. Identification of frequent somatic mutations in inflammatory breast cancer. *Breast Cancer Res Treat.* **163**, 263–272 (2017).
14. Ross, J. S. et al. Comprehensive genomic profiling of inflammatory breast cancer cases reveals a high frequency of clinically relevant genomic alterations. *Breast Cancer Res Treat.* **154**, 155–162 (2015).
15. Bertucci, F. et al. Gene expression profiles of inflammatory breast cancer: correlation with response to neoadjuvant chemotherapy and metastasis-free survival. *Ann. Oncol.* **25**, 358–365 (2014).
16. Lerebours, F. et al. NF-kappa B genes have a major role in inflammatory breast cancer. *BMC Cancer* **8**, 41 (2008).
17. Van Laere, S. et al. Distinct molecular signature of inflammatory breast cancer by cDNA microarray analysis. *Breast Cancer Res Treat.* **93**, 237–246 (2005).
18. Van Laere, S. J. et al. NF-kappaB activation in inflammatory breast cancer is associated with oestrogen receptor downregulation, secondary to EGFR and/or ErbB2 overexpression and MAPK hyperactivation. *Br. J. Cancer* **97**, 659–669 (2007).
19. Marotta, L. L. et al. The JAK2/STAT3 signaling pathway is required for growth of CD44(+)CD24(-) stem cell-like breast cancer cells in human tumors. *J. Clin. Invest.* **121**, 2723–2735 (2011).
20. Van Laere, S. J. et al. Uncovering the molecular secrets of inflammatory breast cancer biology: an integrated analysis of three distinct Affymetrix gene expression datasets. *Clin. Cancer Res.* **19**, 4685–4696 (2013).
21. Bieche, I. et al. Molecular profiling of inflammatory breast cancer: identification of a poor-prognosis gene expression signature. *Clin. Cancer Res.* **10**, 6789–6795 (2004).
22. Allen, S. G. et al. Macrophages enhance migration in inflammatory breast cancer cells via RhoC GTPase signaling. *Sci. Rep.* **6**, 39190 (2016).
23. Lacerda, L. et al. Mesenchymal stem cells mediate the clinical phenotype of inflammatory breast cancer in a preclinical model. *Breast Cancer Res.* **17**, 42 (2015).
24. Wolfe, A. R. et al. Mesenchymal stem cells and macrophages interact through IL-6 to promote inflammatory breast cancer in pre-clinical models. *Oncotarget* **7**, 82482–82492 (2016).
25. Reddy, S. M. et al. Poor response to neoadjuvant chemotherapy correlates with mast cell infiltration in inflammatory breast cancer. *Cancer Immunol. Res.* **7**, 1025–1035 (2019).
26. 1000 Genomes Project Consortium. et al. An integrated map of genetic variation from 1,092 human genomes. *Nature* **491**, 56–65 (2012).
27. Li, H. & Durbin, R. Fast and accurate short read alignment with Burrows-Wheeler transform. *Bioinformatics* **25**, 1754–1760 (2009).
28. McKenna, A. et al. The Genome Analysis Toolkit: a MapReduce framework for analyzing next-generation DNA sequencing data. *Genome Res.* **20**, 1297–1303 (2010).
29. Rimmer, A. et al. G. Integrating mapping- assembly- and haplotype-based approaches for calling variants in clinical sequencing applications. *Nat. Genet.* **46**, 912–918 (2014).
30. Cibulskis, K. et al. Sensitive detection of somatic point mutations in impure and heterogeneous cancer samples. *Nat. Biotechnol.* **31**, 213–219 (2013).
31. Ye, K., Schulz, M. H., Long, Q., Apweiler, R. & Ning, Z. Pindel: a pattern growth approach to detect break points of large deletions and medium sized insertions from paired-end short reads. *Bioinformatics* **25**, 2865–2871 (2009).
32. Sachidanandam, R. et al. Group ISMW. A map of human genome sequence variation containing 1.42 million single nucleotide polymorphisms. *Nature* **409**, 928–933 (2001).
33. Lek, M. et al. Consortium EA. Analysis of protein-coding genetic variation in 60,706 humans. *Nature* **536**, 285–291 (2016).
34. Fu, W. et al. Analysis of 6,515 exomes reveals the recent origin of most human protein-coding variants. *Nature* **493**, 216–220 (2013).
35. Wang, K., Li, M. & Hakonarson, H. ANNOVAR: functional annotation of genetic variants from high-throughput sequencing data. *Nucleic Acids Res.* **38**, e164 (2010).

36. Liu, X., Li, C., Mou, C., Dong, Y. & Tu, Y. dbNSFP v4: a comprehensive database of transcript-specific functional predictions and annotations for human nonsynonymous and splice-site SNVs. *Genome Med.* **12**, 103 (2020).
37. Sirotkin, SmigielskiE. M., Ward, K. & Sherry, M. ST. dbSNP: a database of single nucleotide polymorphisms. *Nucleic Acids Res.* **28**, 352–355 (2000).
38. Landrum, M. J. et al. ClinVar: public archive of relationships among sequence variation and human phenotype. *Nucleic Acids Res.* **42**, D980–D985 (2014).
39. Tate, J. G. et al. COSMIC: the catalogue of somatic mutations in cancer. *Nucleic Acids Res.* **47**, D941–D947 (2019).
40. Olshen, A. B., Venkatraman, E. S., Lucito, R. & Wigler, M. Circular binary segmentation for the analysis of array-based DNA copy number data. *Biostatistics* **5**, 557–572 (2004).
41. Dobin, A. et al. STAR: ultrafast universal RNA-seq aligner. *Bioinformatics* **29**, 15–21 (2013).
42. Anders, S., Pyl, P. T. & Huber, W. HTSeq–a Python framework to work with high-throughput sequencing data. *Bioinformatics* **31**, 166–169 (2015).
43. Love, M. I., Huber, W. & Anders, S. Moderated estimation of fold change and dispersion for RNA-seq data with DESeq2. *Genome Biol.* **15**, 550 (2014).
44. Hanzelmann, S., Castelo, R. & Guinney, J. GSVA: gene set variation analysis for microarray and RNA-seq data. *BMC Bioinforma.* **14**, 7 (2013).
45. Liberzon, A. et al. The Molecular Signatures Database (MSigDB) hallmark gene set collection. *Cell Syst.* **1**, 417–425 (2015).
46. Chen, B., Khodadoust, M. S., Liu, C. L., Newman, A. M. & Alizadeh, A. A. Profiling Tumor Infiltrating Immune Cells with CIBERSORT. *Methods Mol. Biol.* **1711**, 243–259 (2018).
47. Bertucci, F. et al. NOTCH and DNA repair pathways are more frequently targeted by genomic alterations in inflammatory than in non-inflammatory breast cancers. *Mol. Oncol.* **14**, 504–519 (2020).
48. Wang, P., Chen, Y. & Wang, C. Beyond tumor mutation burden: tumor neoantigen burden as a biomarker for immunotherapy and other types of therapy. *Front Oncol.* **11**, 672677 (2021).
49. Ward, J. P., Gubin, M. M. & Schreiber, R. D. The role of neoantigens in naturally occurring and therapeutically induced immune responses to cancer. *Adv. Immunol.* **130**, 25–74 (2016).
50. Bertucci, F. et al. Immune landscape of inflammatory breast cancer suggests vulnerability to immune checkpoint inhibitors. *Oncoimmunology* **10**, 1929724 (2021).
51. Hogan, S. P. et al. Eosinophils: biological properties and role in health and disease. *Clin. Exp. Allergy* **38**, 709–750 (2008).
52. Dajotoy, T. et al. Human eosinophils produce the T cell-attracting chemokines MIG and IP-10 upon stimulation with IFN-gamma. *J. Leukoc. Biol.* **76**, 685–691 (2004).
53. Ito, T. et al. Anti-tumor immunity via the superoxide-eosinophil axis induced by a lipophilic component of Mycobacterium lipomannan. *Int Immunol.* **29**, 411–421 (2017).
54. Liu, L. Y. et al. Generation of Th1 and Th2 chemokines by human eosinophils: evidence for a critical role of TNF-alpha. *J. Immunol.* **179**, 4840–4848 (2007).
55. Grisaru-Tal, S., Itan, M., Klion, A. D. & Munitz, A. A new dawn for eosinophils in the tumour microenvironment. *Nat. Rev. Cancer* **20**, 594–607 (2020).
56. Simon, S. C. S., Utikal, J. & Umansky, V. Opposing roles of eosinophils in cancer. *Cancer Immunol. Immunother.* **68**, 823–833 (2019).
57. Wang, X. et al. EGFR is a master switch between immunosuppressive and immunoactive tumor microenvironment in inflammatory breast cancer. *Sci. Adv.* **8**, eabn7983 (2022).
58. Shi, S., Yoon, D. Y., Hodge-Bell, K., Huerta-Yepez, S. & Hankinson, O. Aryl hydrocarbon nuclear translocator (hypoxia inducible factor 1beta) activity is required more during early than late tumor growth. *Mol. Carcinog.* **49**, 157–165 (2010).
59. Shrivastava, A. et al. An orphan receptor tyrosine kinase family whose members serve as nonintegrin collagen receptors. *Mol. Cell.* **1**, 25–34 (1997).
60. Sasaki, S. et al. DDR2 expression is associated with a high frequency of peritoneal dissemination and poor prognosis in colorectal cancer. *Anticancer Res.* **37**, 2587–2591 (2017).
61. Tsai, M. C. et al. DDR2 overexpression in urothelial carcinoma indicates an unfavorable prognosis: a large cohort study. *Oncotarget* **7**, 78918–78931 (2016).
62. Elsarraj, H. S. et al. Expression profiling of in vivo ductal carcinoma in situ progression models identified B cell lymphoma-9 as a molecular driver of breast cancer invasion. *Breast Cancer Res.* **17**, 128 (2015).
63. Mani, M. et al. BCL9 promotes tumor progression by conferring enhanced proliferative, metastatic, and angiogenic properties to cancer cells. *Cancer Res.* **69**, 7577–7586 (2009).
64. Horejs-Hoeck, J., Hren, A., Mudde, G. C. & Woisetschlager, M. Inhibition of immunoglobulin E synthesis through Fc gammaRII (CD32) by a mechanism independent of B-cell receptor co-cross-linking. *Immunology* **115**, 407–415 (2005).
65. Smith, K. G. & Clatworthy, M. R. FcgammaRIIB in autoimmunity and infection: evolutionary and therapeutic implications. *Nat. Rev. Immunol.* **10**, 328–343 (2010).
66. Gonzalo, S. DNA damage and lamins. *Adv. Exp. Med Biol.* **773**, 377–399 (2014).
67. Cancer Genome Atlas, N. Comprehensive molecular portraits of human breast tumours. *Nature* **490**, 61–70 (2012).
68. Pereira, B. et al. The somatic mutation profiles of 2,433 breast cancers refines their genomic and transcriptomic landscapes. *Nat. Commun.* **7**, 11479 (2016).
69. Wang, Y. et al. GATA-3 controls the maintenance and proliferation of T cells downstream of TCR and cytokine signaling. *Nat. Immunol.* **14**, 714–722 (2013).
70. Kitamura, M. et al. Progression potential of ductal carcinoma in situ assessed by genomic copy number profiling. *Pathobiology* **86**, 92–101 (2019).
71. Shah, S. P. et al. The clonal and mutational evolution spectrum of primary triple-negative breast cancers. *Nature* **486**, 395–399 (2012).
72. Hu, H. et al. PIK3CA mutation confers resistance to chemotherapy in triple-negative breast cancer by inhibiting apoptosis and activating the PI3K/AKT/mTOR signaling pathway. *Ann. Transl. Med.* **9**, 410 (2021).
73. Su, K. et al. Fibrinogen-like protein 2/fibroleukin prothrombinase contributes to tumor hypercoagulability via IL-2 and IFN-gamma. *World J. Gastroenterol.* **14**, 5980–5989 (2008).
74. Adams, R. A., Passino, M., Sachs, B. D., Nuriel, T. & Akassoglou, K. Fibrin mechanisms and functions in nervous system pathology. *Mol. Interv.* **4**, 163–176 (2004).
75. Davalos, D. & Akassoglou, K. Fibrinogen as a key regulator of inflammation in disease. *Semin Immunopathol.* **34**, 43–62 (2012).
76. Mei, Y. et al. Plasma fibrinogen level may be a possible marker for the clinical response and prognosis of patients with breast cancer receiving neoadjuvant chemotherapy. *Tumour Biol.* **39**, 1010428317700002 (2017).
77. Wang, Y. et al. Plasma fibrinogen acts as a predictive factor for pathological complete response to neoadjuvant chemotherapy in breast cancer: a retrospective study of 1004 Chinese breast cancer patients. *BMC Cancer* **21**, 542 (2021).
78. Zhang, X. et al. FGG promotes migration and invasion in hepatocellular carcinoma cells through activating epithelial to mesenchymal transition. *Cancer Manag Res.* **11**, 1653–1665 (2019).
79. Van der Auwera, I. et al. Integrated miRNA and mRNA expression profiling of the inflammatory breast cancer subtype. *Br. J. Cancer* **103**, 532–541 (2010).

80. Matsuda, N. et al. Safety and efficacy of panitumumab plus neoadjuvant chemotherapy in patients with primary HER2-negative inflammatory breast cancer. *JAMA Oncol.* **4**, 1207–1213 (2018).
81. Li, J. et al. Triple-negative subtype predicts poor overall survival and high locoregional relapse in inflammatory breast cancer. *Oncologist* **16**, 1675–1683 (2011).

Acknowledgements

We thank the patients and their families for participating in clinical trial NCT02876107. We thank Amgen for supporting the clinical trial. We thank the staff of the Morgan Welch Inflammatory Breast Cancer Research Program and Clinic for conducting clinical trial NCT02876107. We thank Ms. Stephanie P. Deming (Research Medical Library, The University of Texas MD Anderson Cancer Center) for the expert editorial assistance. This work was supported by the Rare Tumor Initiative as a part of the STrategic Research Initiative DEvelopment (STRIDE) program at The University of Texas MD Anderson Cancer Center. This work was also funded by the Morgan Welch Inflammatory Breast Cancer Research Program and Clinic, the State of Texas Rare and Aggressive Breast Cancer Research Program (NTU), Breast Cancer Research Foundation grants BCRF-22-164 and BCRF-23-164 (NTU), National Institutes of Health grant 1R01CA258523-01A1 (NTU), the Still Water Foundation (Stacy Moulder), and the Winterhof Fund (Stacy Moulder). ARTEMIS data were supported by generous philanthropic contributions to The University of Texas MD Anderson Cancer Center Moon Shots Program™. This work is also supported by the NIH/NCI under award number P30CA016672.

Author contributions

X.W. and L.Z. contributed equally to this work. **Conceptualization**: X.W., L.Z., L.W.C., N.T.U., A.F., R.T.I.T. **Methodology and experimentation**: A.V., S.K., R.T.I.T., T.S., S.S. **Data analysis**: L.Z., X.S., X.W., M.K., R.C., J.Z., S.E.W. **Administrative, technical, or material support**: L.W.C., A.A., S.B., W.A.W., C.Y., H.L. **Study supervision**: N.T.U., C.Y. **Writing, review, and/or revision of the manuscript**: X.W., L.Z., L.W.M.L., D.T., A.N., N.T.U. All authors read and approved the final manuscript.

Competing interests

C.Y. has received research support (to the institution) from Amgen, Merck, Genentech, and GSK. N.T.U. holds consulting roles with the following companies: AstraZeneca Pharmaceuticals LP (USA and UK), Bayer AG, Bristol Myers Squibb Company, Carna Biosciences, Inc., CytoDyn Inc., Daiichi Sankyo Co., Ltd., Eisai Co., Ltd., Eli Lilly and Company, Genentech, Inc., Genomic Health, Inc., Gilead Sciences, Inc., Lavender Health, OncoCyte Corporation, Pear Bio, Peptilogics, Inc., Pfizer Inc., Phoenix Molecular Designs, Preferred Medicine, Carisma Therapeutics, Inc., Sysmex Corporation, Takeda Pharmaceutical Company Limited (Japan), and Unitech Medical, Inc. N.T.U. holds consulting roles with the following companies: AstraZeneca Pharmaceuticals LP (USA and UK), Bayer AG, Bristol Myers Squibb Company, Carna Biosciences, Inc., CytoDyn Inc., Daiichi Sankyo Co., Ltd., Eisai Co., Ltd., Eli Lilly and Company, Genentech, Inc., Genomic Health, Inc., Gilead Sciences, Inc., Lavender Health, OncoCyte Corporation, Pear Bio, Peptilogics, Inc., Pfizer Inc., Phoenix Molecular Designs, Preferred Medicine, Carisma Therapeutics, Inc., Sysmex Corporation, Takeda Pharmaceutical Company Limited (Japan), and Unitech Medical, Inc. N.T.U. has ownership of stock: Pear Bio and Phoenix Molecular Designs. N.T.U. holds speaker or preceptorship roles with the following companies: Daiichi Sankyo Co., Ltd., Kyowa Kirin Co., Ltd., Pfizer Inc., AstraZeneca Pharmaceuticals LP, Total Health Conferencing, and Eli Lilly and Company. N.T.U. has research agreements in place with the following companies: AnHeart Therapeutics Inc., Eisai Co., Ltd., Gilead Sciences, Inc., Phoenix Molecular Designs, Daiichi Sankyo, Inc., Puma Biotechnology, Inc., Merck Co., Oncolys BioPharma Inc., OBI Pharma Inc., ChemDiv, Inc., Tolero Pharmaceuticals, Inc., and VITRAC Therapeutics, LLC. All other authors have no relevant conflict of interest disclosures.

Additional information

Supplementary information The online version contains supplementary material available at https://doi.org/10.1038/s41698-024-00729-0.

Correspondence and requests for materials should be addressed to Xiaoping Wang or Naoto T. Ueno.

Rare Tumor Initiative Team

Ahmed N. Al Rawi[4], Claudio A. Arrechedera[4], Kimberly S. Ayers[4], Claudia Alvarez Bedoya[4], Elizabeth Burton[4], Connie A. Chon[4], Randy Aaron Chu[4], Shadarra D. Crosby[4], Jonathan Do[4], Cibelle Freitas Pinto Lima[4], Szu-Chin Fu[4], Andy Futreal[4], Ana L. Garcia[4], Celia Garcia-Prieto[4], Swati Gite[4], Curtis Gumbs[4], Kristin J. Hargraves[4], Meng He[4], Chacha Horombe[4], Heladio P. Ibarguen[4], Stacy Jackson[4], Jeena Jacob[4], Mei Jiang[4], Isha Khanduri[4], Walter K. Kinyua[4], Xiaogang Wu[4], Wenhua Lang[4], Latasha D. Little[4], Wei Lu[4], Saradhi Mallampati[4], Mary Gertrude T. Mendoza[4], Funda Meric-Bernstam[4], Mohammad Moustaf Mohammad[4], Mario Luiz Marques Piubelli[4], Sabitha Prabhakaran[4], Kenna R. Shaw[4], Xingzhi Song[4], Ping Song[4], Xiaofei Song[4], Sandesh Subramanya[4], Baohua Sun[4], Shumaila Virani[4], Wanlin Wang[4], Ignacio Wistuba[4], Le-Petross Huong[1,7], Mingchu Xu[4], Jianhua Zhang[4], Qingxiu C. Zhang[4] & Shanyu Zhang[4]